Tribological characterization of a hip prosthesis in Si3N4-TiN ceramic composite made with Electrical Discharge Machining (EDM)

Available online at www.sciencedirect.com

ScienceDirect

Procedia Structural Integrity 33 (2021) 469–481

Structural Integrity Procedia

www.elsevier.com/locate/procedia

IGF26 - 26th International Conference on Fracture and Structural Integrity

Tribological characterization of a hip prosthesis in Si3N4-TiN ceramic composite made with Electrical Discharge Machining (EDM)

Danilo D'Andrea[a], Alessandro Pistone[a], Giacomo Risitano[a], Dario Santonocito[a], Lorenzo Scappaticci[b], Fabio Alberti[a]*

[a]University of Messina, Department of Engineering, Contrada di Dio, 98166 Messina, Italy
[b]Allimep srl, Via dell'acciaio 7, 06134 Ponte Felcino (PG), Italy

Abstract

In this work, the friction and wear behavior in hip prosthesis made of Si_3N_4-TiN ceramic composite were evaluated by tribological tests in order to estimate the prosthesis life. The innovation consists in the use of Electrical Discharge Machining (EDM) for the realization of the hip prosthesis. This was allowed using TiN as a dopant of the ceramic matrix which confer electrical conductivity properties to the composite, necessary in order to use the EDM. The Coefficient of Friction (CoF) and Wear Rate (WR) were evaluated through experimental tribological tests using a tribometer with Pin on Disk (PoD) configuration. The experimental results were used for the calibration of the Archard wear model adopted to simulate the wear process between pin and disk. Finally, after calibrating the wear model, numerical analysis was performed to evaluate the wear of the material and the life cycle of the hip prosthesis.

Keywords: Hip prosthesis; Electrical Discharge Machining; Life cycle estimation.

1. Introduction

Prosthetic surgery has revolutionized the clinical course of patients suffering from joint arthritis, rheumatoid arthritis, post-traumatic arthrosis, congenital dysplasia, and bone necrosis on a vascular basis.

* Corresponding author. Tel.: +39 3385661220.
E-mail address: fabio.alberti@unime.it

10.1016/j.prostr.2021.10.054

However, many problems that lead to the deterioration of a prosthesis are due to friction and wear of the materials used in the joint [1,2]. The problems of friction and wear in hip prosthesis, as well as in other types of mechanical joint, have been studied by many authors [3–7] in order to quantify the effects on the quality, reliability and durability of the prostheses. The hip joint is an arthrosis consisting of the acetabulum of the coax bone and the femur head. It joins the femur to the hip bone by relating the acetabulum with the femur head. The study of this type of coupling is very important for studying the wear effects on a hip prosthesis. To optimize the life of the prosthesis it is very important to minimize the coefficient of friction that is generated between the different materials. In fact, during operation, the less rigid part of the prosthesis wears and releases debris into the body, even in the order of micrometers, which cause reactions in the body [8–11]. Oldenburg et al. [12] have studied the effect of the deterioration of the femoral prosthesis on a 55-year-old man with a total hip replacement. In particular, clinical examinations revealed for the first-time hypothyroidism, peripheral neuropathy and cardiomyopathy due to the high concentrations of cobalt. For this reason, prostheses with metal-metal coupling are not made. In fact, this coupling has one of the greatest coefficients of friction, which causes rapid deterioration of the prosthesis and the greater presence of debris inside the human body. Better behavior in terms of friction and wear is obtained by using a metal-UHMWPE (ultra-high molecular weight polyethylene), Ceramic-UHMWPE and Ceramic-Ceramic coupling [13–17]. Thanks to their great potential, studies regarding the application of ceramic composites have intensified in recent years [18–20]. These are "doped" ceramics, i.e. consisting of a ceramic matrix and a second metal phase dissolved on it. The presence of the metal phase modifies some characteristics of the material, making it usable also for unconventional mechanical processing [21]. Excellent results have been obtained in the biomedical field, where they have shown good mechanical properties. [22–25]. Recent works are related to the realization of hip prosthesis through additive manufacturing technique [26]; moreover, the development of the Artificial Intelligence and Machine learning algorithm for the determination of the human body center of mass [27], could bring good insight for the exactly load distribution on the prosthesis.

In this paper the tribological properties of a hip prosthesis made of Si_3N_4-TiN ceramic composite have been studied. The innovative aspect concerns the use of an unconventional technique such as Electrical Discharge Machining (EDM) for the realization of the prosthesis in Si_3N_4-TiN. This was allowed using TiN as a dopant of the ceramic matrix, which allowed to confer properties of electrical conductivity to the composite, necessary in order to use the EDM [28]. To evaluate the friction coefficient of the Si_3N_4-TiN, a tribological tests were performed using a tribometer with pin on disk (POD) [29] configuration. After the tribological tests, the failure analysis and numerical analysis were performed in order to evaluate the wear of the material and the life cycle of the prosthesis. The finite element hip model consists in the coupling between the acetabular cup and the femur head. The lubrication and roughness of the contact surface has been considered through a friction coefficient evaluated from the tribological tests. A complete 3D physiological gait loading and kinematic motions of normal walking has been considered in order to correctly apply load and rotation condition to the finite element model. From the simulation results, the prosthesis life has been evaluated considering the volume loss due to wear for one year of gait. The results have been finally compared with literature study and clinical cases, showing a good agreement with them.

Nomenclature

μ	Friction coefficient
H	Material hardness [MPa]
K	Archard wear coefficient
W	Wear rate [m^3/s]
L	Sliding distance [m]
p	Contact pressure [MPa]
v	Sliding velocity [m/s]
m	Pressure coefficient
n	Velocity coefficient
MRR	Material Removal Rate [m^3/s]
R	Pin head radius [m]

d_{mean}	Pin head mean diameter [m]

2. Materials and Methods

2.1. Sample preparation

The preparation of the specimens and pins for carrying out the tribological tests was achieved by EDM technique. As for the discs, these were made starting from a Si_3N_4-TiN billet with a diameter of 30 mm (see Fig. 1).

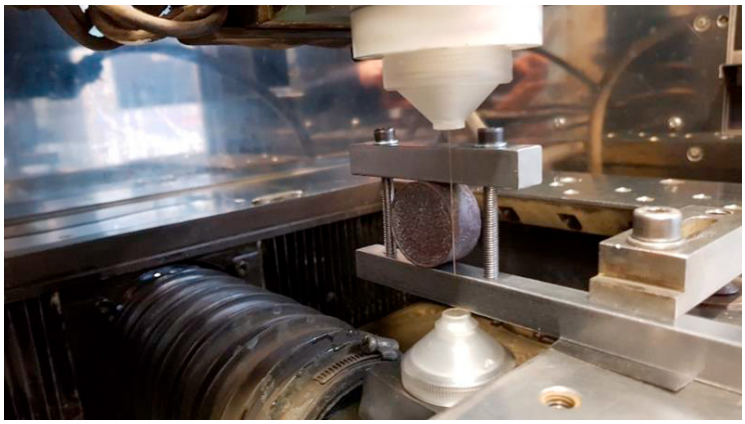

Fig. 1 Production of discs by cutting with EDM technique.

The samples obtained have a diameter of 30 mm, a thickness of 5 mm and roughness of the machined surface equal to 2.67 µm (see Fig. 2a). Since the roughness is too high to perform the tribological test, it is necessary to perform a surface polishing with a 600 µm sandpaper. After machining, the surface roughness is approximately R_a = 0.42 µm (see Fig. 2b).

(a) **(b)**

Fig. 2 a) Surface polished with 600 µm sandpaper b) Raw surface after EDM processing

The processing of the pins for the tribological test involves the use of both EDM technologies: the first phase is to obtain the cylindrical body of the pins through the use of the wire EDM machine, while the second phase is for making the hemispherical head on a plunge EDM machine (see Fig. 3a). From the processing, we obtain a smooth and homogeneous hemisphere without particular surface discontinuities. From the values set by default on the machine, a surface roughness of Ra = 0.8 µm is obtained (see Fig. 3b).

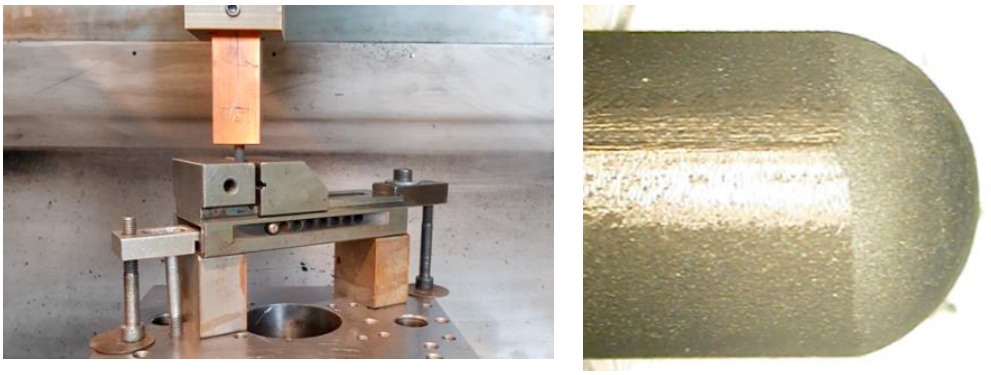

(a) (b)

Fig. 3 a) Machining of the hemispherical head of the pin b) Hemispherical head of the pin

2.2. Tribological test

For the tribological test, a tribometer with POD configuration was used (see Fig. 4). The system consists of:

- a guided mandrel that supports the pin holder;
- a mandrel needed to fix the rotating disc;
- a lever device to keep the pin fixed;
- a device to allow the specimen to be forced against the rotating disc with controlled load.

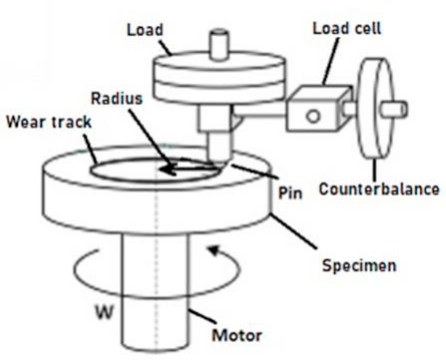

Fig. 4 Tribometer in Pin on Disk configuration

The system is equipped with a load cell for measuring the friction force. A variable speed motor capable of maintaining constant speed during the test rotates the plane containing the disc. Tribological tests were carried out using the parameters shown in Table 1.

Table 1. Tribological test parameters

Vertical load (N)	Distance (*m*)	Rotation speed (rpm)	Time (s)	Lubrication
10	22000	350	150	Full

As reported in Table 1, the tests were performed in a full lubricating bath, which allows to simulate the joint friction coefficient in the synovial fluid. To simulate this behavior, fetal bovine serum was chosen as the lubricant. Its viscosity, in fact, allows simulating the hip joint, the lubrication of the contact part and the cleaning of debris generated by wear.

Failure analysis was performed to characterize the behavior and the wear rate of the specimens, with the use of optical microscope (OM) and confocal microscope.

2.3. POD numerical analysis

In order to predict the wear rate of the Si_3N_4-TiN composite obtained by EDM process, a finite element model was developed in Ansys® Workbench 19.2 for the POD test. Both the geometry of the disk and pin were modelled; in particular, for the latter only the spherical part was considered, neglecting the cylindrical body. High-order 20-node SOLID186 element was adopted, and after a convergence analysis, the pin was modelled with 284 elements while the disk with 129 elements. The materials properties of the composite material Si_3N_4-TiN, as reported in Table. 2, were adopted.

Table 2 Material properties of the composite material Si_3N_4-TiN

Properties	Value	Unit
Density	4010	kg/m^3
Isotropic Secant Coefficient of Thermal expansion	9.4E-06	K^{-1}
Young's Modulus	3.41E+05	MPa
Poisson's ratio	0.31	
Tensile Yield Strength	350	MPa
Tensile Ultimate Strength	370	MPa
Micro hardness	14.7	GPa

A frictional contact type between pin and disk was simulated adopting the disk as the target surface, modelled with TARGE170 elements, while the pin as the contact surface with CONTA174 elements. The detection method was set to "Nodal-Normal to Target" and the "Adjust to touch" option for the surfaces was enabled prior to run the simulations. The Archard wear model was adopted to simulate the wear process between pin and disk, according to Eq. 1.

$$w=\frac{K}{H}p^m v^n \tag{1}$$

Where w is the wear rate; K the Archard wear coefficient; H the material hardness (in MPa); p the contact pressure; v the sliding velocity; m and n pressure and velocity coefficient respectively. The wear coefficient K has been estimated from the experimental Pin On Disk test. At the first, through a microscopically examination, the track size of the pin (mean diameter d_{mean}) has been calculated, as shown in Fig. 5.

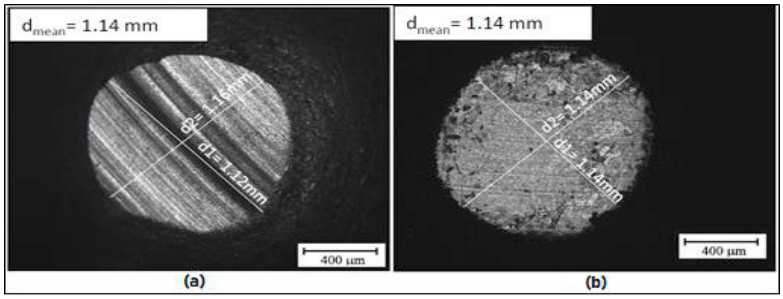

Fig. 5 a) Track size calculation in Test A; b) Microscopy of the track size of the pin relating to Test B.

Assuming the geometry of the pin head perfectly spherical with radius R = 3 mm, experimentally calculated, the Archard wear coefficient K can be estimated as follow:

$$r = \frac{d_{mean}}{2} \tag{2}$$

$$h = R - \sqrt{R^2 - r^2} \tag{3}$$

$$V = \frac{\pi h}{6}\left(3r^2 + h^2\right) = 0.0279 \text{ mm}^3 \tag{4}$$

$$K = \frac{VH}{FL} = 2.03 \cdot 10^{-5} \tag{5}$$

The regime conditions were simulated, adopting a vertical load on the pin equal to 10 N and angular velocity of the disk equal to 25 rad/s (Fig. 6)

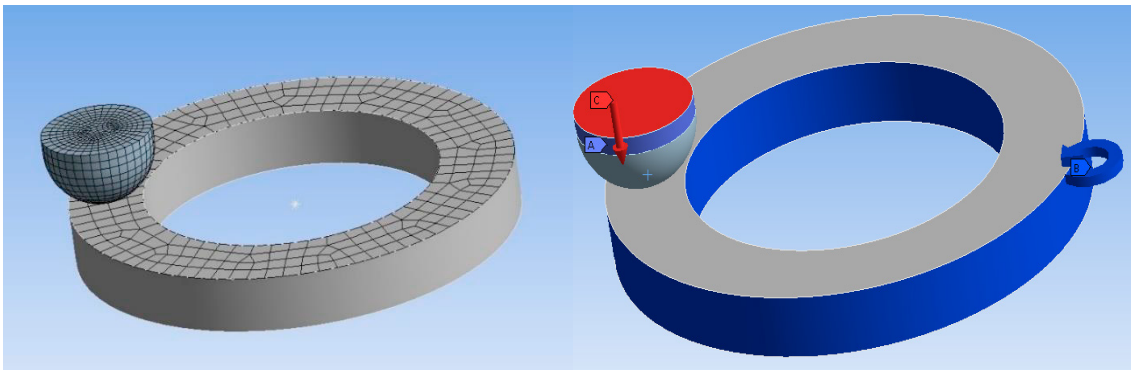

(a) **(b)**

Fig. 6 a) Pin On Disk Finite Element model b) Load and constrain condition of the test

2.4 Hip prosthesis numerical analysis

The hip prosthesis model adopted for the numerical analysis is the Charnley prosthesis model. The prosthesis prototype was designed with the computer support of Cimatron™ CAD, as shown in Fig. 7.

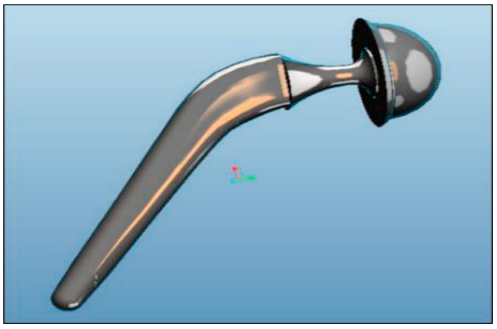

Fig. 7 Charnley prosthesis prototype

A typical gait cycle [30] has been considered in the model, which basically consist in a stance phase and swing phase (Fig. 8).

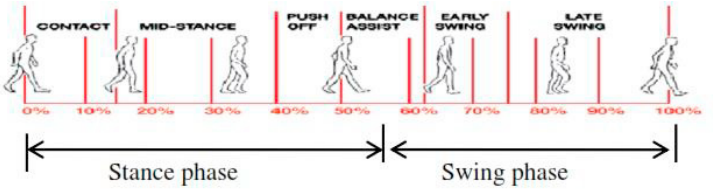

Fig. 8 Typical gait cycle considered in FE analysis [30]

From the gait cycle, load and rotation condition have been evaluated, as shown in Fig. 9.

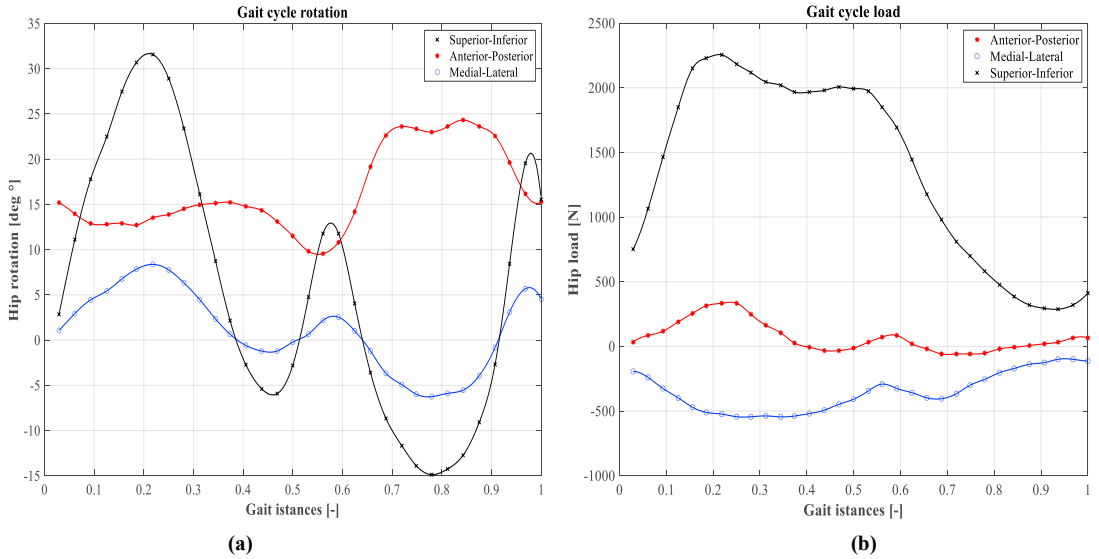

Fig. 9 a) Gait cycle rotation b) Gait cycle load [30]

In order to minimize the computational time, only the femural head and acetabular cup coupling has been considered. Also in this case, frictional contact type between femural head and acetabular cup was simulated, adopting the acetabular cup as the target surface. Both geometries have been meshed using "Automatic method", resulting in a fully 3D Tetra elements mesh. The detection method was set to "Nodal-Normal to Target" and the "Adjust to touch" option for the surfaces was enabled prior to run the simulations. In Fig. 10 is shown the FE element model of the prosthesis with load and rotation condition.

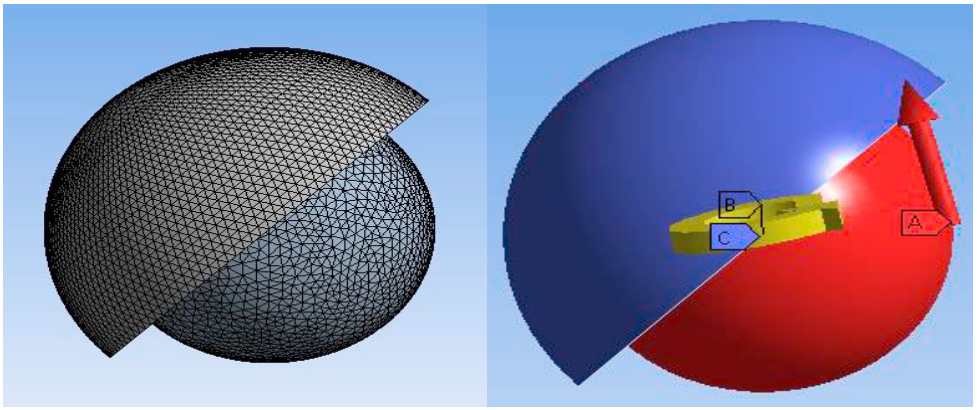

(a) (b)

Fig. 10 a) Hip prosthesis Finite Element model b) Load and costrain condition

3. Results and Discussions

To evaluate the friction coefficient of the Si_3N_4-TiN ceramic composite, several tribological tests (5 tests) were carried out according to the specifications shown in Table 1 and in accordance with the relevant scientific literature [28].

Figures 11a and 11b shows the trend of the coefficient of friction as a function of the distance. It should be noted that only two trends have been explained, as they are the most representative of the tribological behavior of the Si_3N_4-TiN - Si_3N_4-TiN contact. By analyzing the figures, it is possible to note that both cases show a similar behavior characterized by a region with a low friction coefficient, a transition zone and finally a region with a higher friction coefficient.

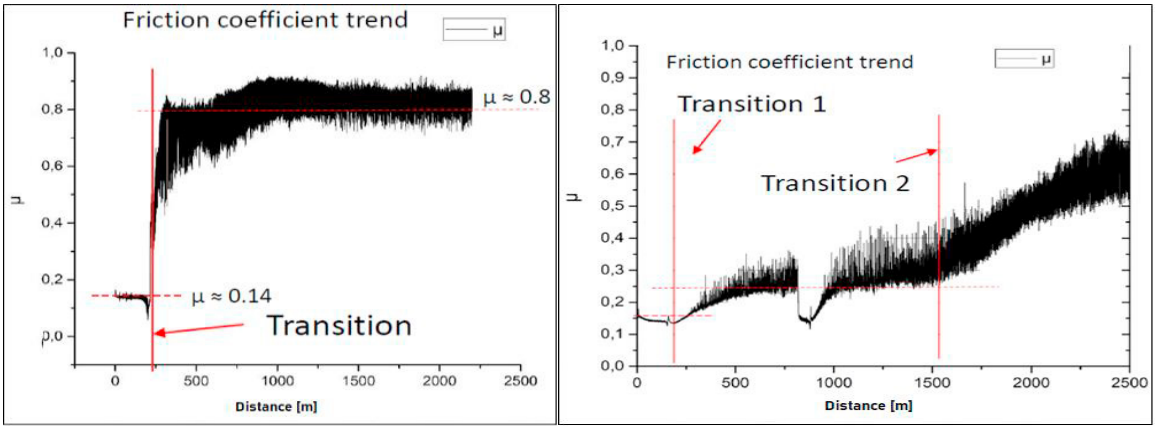

(a) (b)

Fig. 11 Friction coefficient as a function of the distance. a) Test A b) Test B.

In test A, during the first 250 m of sliding, the values assumed by the friction coefficient oscillate around the average value μ = 0.139. This result is similar to that obtained from a test between ceramic materials commonly used for the construction of prostheses such as alumina and zirconia. Furthermore, it is perfectly in line with the results obtained by Bucciotti et al.[28], who carried out the test with a Si3N4-TiN ceramic composite disc placed in contact

with a spherical Alumina pin. After 250 m, however, the coefficient undergoes a sharp variation, rapidly increasing up to the value of μ= 0.8.

It is possible to explain the behavior of specimen A by analyzing the wear track obtained by optical microscope (see Fig. 12a and 12b) and confocal microscopy (see. Fig.13). In the two microscopies, shown in Figures. 12a and 12b, it is possible to note that the track has a larger area than that relating to the initial contact.

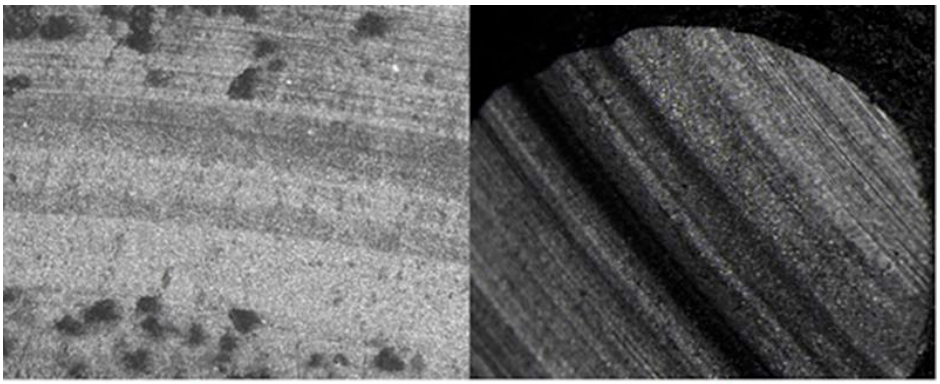

Fig. 12 a) Track on the sample surface at 100x b) Track on the pin surface at 100x

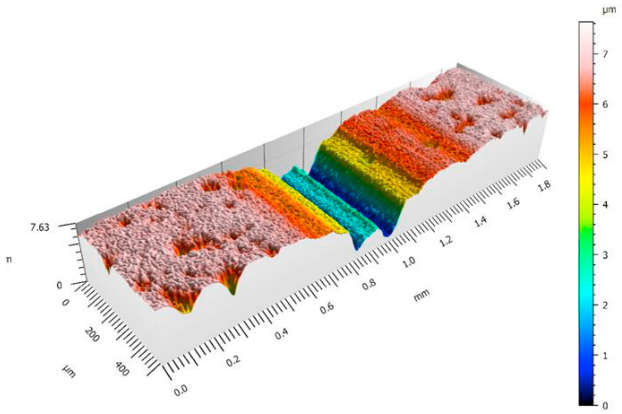

Fig. 13 Confocal microscopy of the wear track after the tribological test

Due to friction and wear, the surface flattens itself by changing the contact area from a single point to a circular section. In this way, the sliding surface between the two specimens is greater and generates an increase in the wear of the disc and the tip of the Pin. However, the aspect that could be more decisive is that relating to lubrication. In the first part of the test, the coupling is well lubricated, the contact surfaces generate a very low friction coefficient and wear is practically zero. When the specimens begin to deform, the bovine serum accumulates debris and the lubrication begins to progressively decrease until the coupling is practically dry. The final value assumed by the friction coefficient corresponds to that obtained from a tribological test between ceramic materials in a dry condition.

In test B, however, the trend of the friction coefficient highlights two clearly visible transition areas. Up to 250 m of sliding, the friction coefficient remains stable at values comparable with test A (0.155). After 250 m it undergoes a slow transition which leads to the stabilization of the CoF values of about 0.24 until reaching 1500 m. The second

transition occurs at this point of the slip, where the values of the friction coefficient progressively increase up to the value of 0.7. The lubrication effect in this case is much more effective than in the previous case and allows keeping the CoF at lower values.

3.1. Pin on Disk wear model

Finite element simulations of the POD test have been carried out for time equal to 1s order to verify a linear relationship between the volume of material removed and the sliding distance. The assumed CoF between the pin and the disc has been set to μ= 0.14, similar to the previous experimental POD tests. As it is possible to note from Fig. 14a the linear assumption between the wear volume and time, can be confirmed and the Material Removal Rate (MRR) can be easily estimated as the ratio between the removed volume and the sliding time. The same linear relation can be noticed between the sliding distance and time (Fig. 14b).

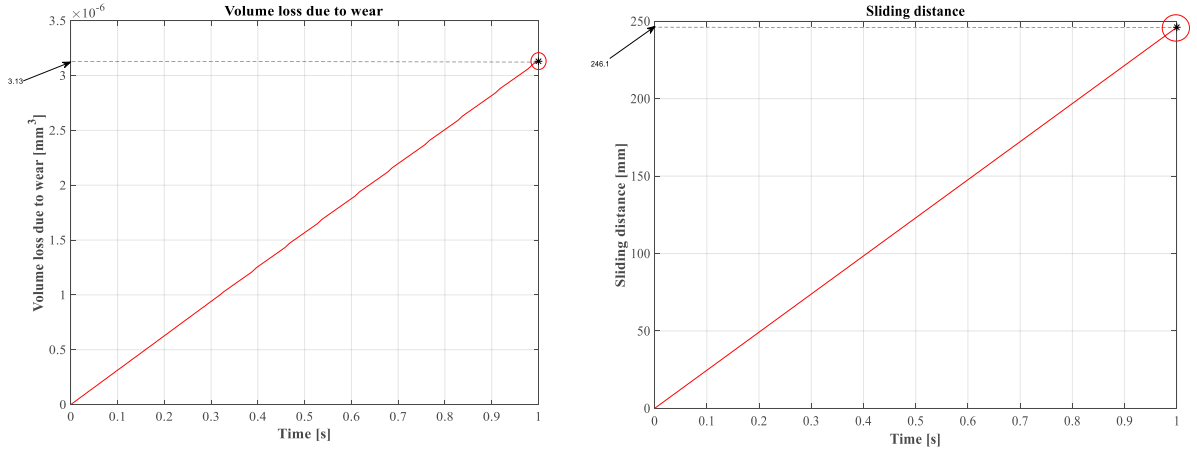

Fig. 14 a) Volume loss due to wear vs. Time b) Sliding distance vs. Time

In Table 3 is reported the MRR for the simulation. Given the linearity between the wear volume and the test time, it is possible to estimate the overall wear volume for the complete POD test, overcoming a complete FE simulation, by means of a simple proportion. Table 3 also reports the prediction for a complete POD test, i.e. the calibration of the Archard wear model (m and n exponent), with a sliding distance of 2200 m and the corresponding experimental data.

Table 3 Calibration of the Archard wear model

	n speed	m pressure	MRR $[mm^3/s]$	Sliding distance [mm]	MRR $[mm^3/m]$	Pin travel [m]	V_{tot} $[mm^3]$	Error [%]
Experimental						2200	0.0279	
FE Calibration	0	2.186	$3.13 \cdot 10^{-6}$	246.1	$1.27 \cdot 10^{-5}$		0.028	0.09

3.2 Hip prosthesis life estimation

After the calibration of the Archard wear model, a numerical analysis has been performed in order to estimate the prosthesis life. In particular, from the simulation results, the volume loss due to wear, referred to one gait cycle, has been evaluated, as shown in Fig. 15.

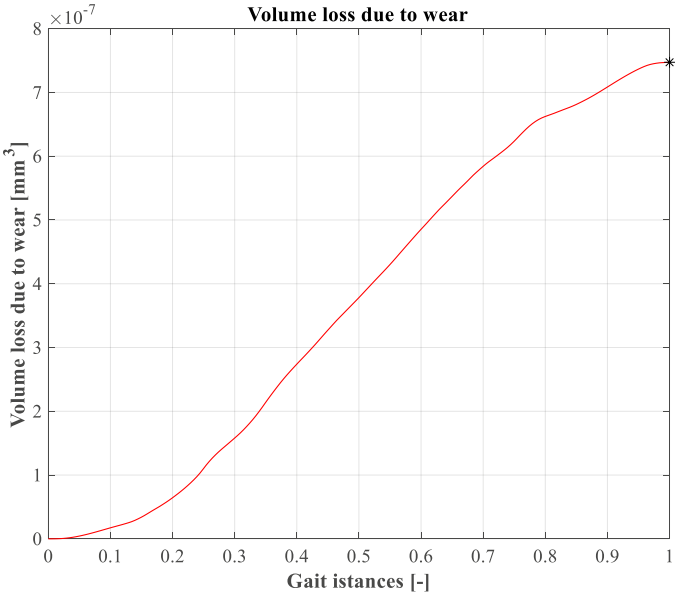

Fig. 15 Volume loss due to wear for one gait cycle

Finally, the obtained result has been related to 10^6 gait cycles, which correspond to one year of gate:

$$W=\frac{7.47\cdot10^{-7}\ \text{mm}^3}{\text{cycles}}\cdot10^6\text{cycles}=0.74\ \frac{\text{mm}^3}{\text{year}} \tag{6}$$

4. Conclusions

Through tribological tests, the friction coefficient for ceramic-on-ceramic coupling has been evaluated and implemented to the numerical analysis. The wear process has been studied with the Archard wear model and the calibration has been performed through Pin On Disk tribological test.

The comparison between the experimental removed volume and the numerical one, shows a high accuracy calibration with low error value. After the calibration of the wear model and the evaluation of the friction coefficient, numerical analysis has been performed in order to estimate the prosthesis life, in terms of volume loss due to wear per year. The EDM technique allows to realize complex geometry with respect to conventional technique, maintaining a good surface finishes and roughness. Hence, this technique is also suitable for the realization of more complex geometries, resulting, for example, from a topological optimization. Considering the good mechanical properties in biomedical fields, the "doped" ceramic could be a valid alternative with respect to the conventional materials. Moreover, the simulation results show that is possible to obtain remarkable results also with a non-linear wear model. This is confirmed by the results comparison with clinical studies and literature review.

References

[1] M. Fellah, M. Labaiz, O. Assala, L. Dekhil, A. Iost, Tribological behavior of biomaterials for total hip prosthesis, Trends Biomater. Artif. Organs. 29 (2015) 22–30.

[2] V. Banchet, V. Fridrici, J.C. Abry, P. Kapsa, Wear and friction characterization of materials for hip prosthesis, Wear. 263 (2007) 1066–1071. https://doi.org/10.1016/j.wear.2007.01.085.

[3] H. McKellop, I. Clarke, K. Markolf, H. Amstutz, Friction and wear properties of polymer, metal, and ceramic prosthetic joint materials evaluated on a multichannel screening device, J. Biomed. Mater. Res. 15 (1981) 619–653. https://doi.org/10.1002/jbm.820150503.

[4] A. Unsworth, R.M. Hall, I.C. Burgess, B.M. Wroblewski, R.M. Streicher, M. Semlitsch, Frictional resistance of new and explanted artificial hip joints, Wear. 2 (1995) 226–231.

[5] M.P. Gispert, A.P. Serro, R. Colaço, B. Saramago, Friction and wear mechanisms in hip prosthesis: Comparison of joint materials behaviour in several lubricants, Wear. 260 (2006) 149–158. https://doi.org/10.1016/j.wear.2004.12.040.

[6] V.O. Saikko, A three-axis hip joint simulator for wear and friction studies on total hip prostheses, Proc. Inst. Mech. Eng. Part H J. Eng. Med. 210 (1996) 175–185. https://doi.org/10.1243/PIME_PROC_1996_210_410_02.

[7] J.L. Tipper, P.J. Firkins, A.A. Besong, P.S.M. Barbour, J. Nevelos, M.H. Stone, E. Ingham, J. Fisher, Characterisation of wear debris from UHMWPE on zirconia ceramic, metal-on-metal and alumina ceramic-on-ceramic hip prostheses generated in a physiological anatomical hip joint simulator, Wear. 250 (2001) 120–128.

[8] Y. Matsuda, T. Yamamuro, R. Kasai, Y. Matsusue, H. Okumura, Severe metallosis due to abnormal abrasion of the femoral head in a dual bearing hip prosthesis: A case report, J. Arthroplasty. 7 (1992) 439–445.

[9] D.L. Back, D.A. Young, A.J. Shimmin, How do serum cobalt and chromium levels change after metal-on-metal hip resurfacing?, Clin. Orthop. Relat. Res. 438 (2005) 177–181.

[10] J.J. Jacobs, A.K. Skipor, L.M. Patterson, N.J. Hallab, W.G. Paprosky, J. Black, J.O. Galante, Metal release in patients who have had a primary total hip arthroplasty. A prospective, controlled, longitudinal study, JBJS. 80 (1998) 1447–1458.

[11] H.G. Seiler, H. Sigel, A. Sigel, Handbook on toxicity of inorganic compounds, (1988).

[12] M. Oldenburg, R. Wegner, X. Baur, Severe Cobalt Intoxication Due to Prosthesis Wear in Repeated Total Hip Arthroplasty, J. Arthroplasty. 24 (2009) 825.e15-825.e20. https://doi.org/10.1016/j.arth.2008.07.017.

[13] T. Roy, D. Choudhury, S. Ghosh, A. Bin Mamat, B. Pingguan-Murphy, Improved friction and wear performance of micro dimpled ceramic-on-ceramic interface for hip joint arthroplasty, Ceram. Int. 41 (2015) 681–690. https://doi.org/10.1016/j.ceramint.2014.08.123.

[14] M. Mazzocchi, D. Gardini, P.L. Traverso, M.G. Faga, A. Bellosi, On the possibility of silicon nitride as a ceramic for structural orthopaedic implants. Part II: Chemical stability and wear resistance in body environment, J. Mater. Sci. Mater. Med. 19 (2008) 2889–2901. https://doi.org/10.1007/s10856-008-3437-y.

[15] B. Derbyshire, J. Fisher, D. Dowson, C. Hardaker, K. Brummitt, Comparative study of the wear of UHMWPE with zirconia ceramic and stainless steel femoral heads in artificial hip joints, Med. Eng. Phys. 16 (1994) 229–236.

[16] P. Kumar, M. Oka, K. Ikeuchi, K. Shimizu, T. Yamamuro, H. Okumura, Y. Kotoura, Low wear rate of UHMWPE against zirconia ceramic (Y-PSZ) in comparison to alumina ceramic and SUS 316L alloy, J. Biomed. Mater. Res. 25 (1991) 813–828.

[17] F. Platon, P. Fournier, S. Rouxel, Tribological behaviour of DLC coatings compared to different materials used in hip joint prostheses, Wear. 250 (2001) 227–236.

[18] G.S. Matharu, J. Daniel, H. Ziaee, D.J.W. McMinn, Failure of a novel ceramic-on-ceramic hip resurfacing prosthesis, J. Arthroplasty. 30 (2015) 416–418.

[19] G. Pezzotti, K. Yamada, S. Sakakura, R.P. Pitto, Raman spectroscopic analysis of advanced ceramic composite for hip prosthesis, J. Am. Ceram. Soc. 91 (2008) 1199–1206.

[20] G. Pezzotti, K. Yamada, A.A. Porporati, M. Kuntz, K. Yamamoto, Fracture toughness analysis of advanced ceramic composite for hip prosthesis, J. Am. Ceram. Soc. 92 (2009) 1817–1822.

[21] D. Hanaoka, Y. Fukuzawa, C. Ramirez, P. Miranzo, M.I. Osendi, M. Belmonte, Electrical discharge machining of ceramic/carbon nanostructure composites, Procedia CIRP. 6 (2013) 95–100.

[22] M.F. Morks, A. Kobayashi, Development of ZrO2/SiO2 bioinert ceramic coatings for biomedical application, J. Mech. Behav. Biomed. Mater. 1 (2008) 165–171.

[23] E. Kalantari, S.M. Naghib, N.J. Iravani, R. Esmaeili, M.R. Naimi-Jamal, M. Mozafari, Biocomposites based on hydroxyapatite matrix reinforced with nanostructured monticellite (CaMgSiO4) for biomedical application: synthesis, characterization, and biological studies, Mater. Sci. Eng. C. 105 (2019) 109912.

[24] C. Petit, L. Montanaro, P. Palmero, Functionally graded ceramics for biomedical application: Concept, manufacturing, and properties, Int. J. Appl. Ceram. Technol. 15 (2018) 820–840.

[25] M. Dziadek, E. Stodolak-Zych, K. Cholewa-Kowalska, Biodegradable ceramic-polymer composites for biomedical applications: A review, Mater. Sci. Eng. C. 71 (2017) 1175–1191.

[26] F. Cucinotta, E. Guglielmino, G. Longo, G. Risitano, D. Santonocito, F. Sfravara, Topology optimization additive manufacturing-oriented for a biomedical application, Springer International Publishing, 2019. https://doi.org/10.1007/978-3-030-12346-8_18.

[27] D. D'andrea, F. Cucinotta, F. Farroni, G. Risitano, D. Santonocito, L. Scappaticci, Development of machine learning algorithms for the determination of the centre of mass, Symmetry (Basel). 13 (2021) 1–16. https://doi.org/10.3390/sym13030401.

[28] F. Bucciotti, M. Mazzocchi, A. Bellosi, Perspectives of the Si3N4-TiN ceramic composite as a biomaterial and manufacturing of complex-shaped implantable devices by electrical discharge machining (EDM), J. Appl. Biomater. Biomech. 8 (2010) 28–32.

[29] A. Senatore, G. Risitano, L. Scappaticci, D. D'andrea, Investigation of the tribological properties of different textured lead bronze coatings under severe load conditions, Lubricants. 9 (2021) 1–14. https://doi.org/10.3390/lubricants9040034.

[30] M.S. Uddin, L.C. Zhang, Predicting the wear of hard-on-hard hip joint prostheses, Wear. 301 (2013) 192–200. https://doi.org/10.1016/j.wear.2013.01.009.